Hindawi Publishing Corporation
Journal of Nanomaterials
Volume 2014, Article ID 130539, 7 pages
http://dx.doi.org/10.1155/2014/130539

Research Article

Electrospun ZnO/Bi_2O_3 Nanofibers with Enhanced Photocatalytic Activity

Yingying Yang,[1] Lingling Xu,[1] Chunyan Su,[2] Jixin Che,[3] Wenjun Sun,[1] and Hong Gao[1]

[1] *Key Laboratory of Photonic and Electric Bandgap Materials of Ministry of Education, School of Physics and Electronic Engineering, Harbin Normal University, Harbin 150025, China*
[2] *Department of Physics, Harbin University, Harbin 150086, China*
[3] *The Aviation University of Air Force, Changchun 130022, China*

Correspondence should be addressed to Lingling Xu; xulingling_hit@163.com

Received 20 September 2013; Revised 3 January 2014; Accepted 11 January 2014; Published 3 March 2014

Academic Editor: Alireza Khataee

ZnO/Bi_2O_3 nanofibers were synthesized by a simple electrospinning method and both the UV and visible light responsive photocatalytic properties were studied by the decolorization of RhB dye. Thermogravimetric analysis/differential thermal analysis (TGA-DTA), X-ray diffraction (XRD), scanning electron microscope (SEM), and UV-vis diffuse reflectance spectra (DRS) were employed to study the structure, morphology, and optical properties of the ZnO/Bi_2O_3 nanofibers, respectively. The relationship between the ZnO/Bi_2O_3 ratio and photocatalytic activity was also studied, and the composite with a molar ratio of 23 : 1 demonstrated the best activity under both excitations. The photocatalytic mechanisms for the composite fibers can be described as the direct photocatalysis under UV excitation and photosensitation for visible light irradiation. The enhanced photocatalytic activities can be ascribed to the effective electron-hole pairs separation that leads to the promoted photocatalytic efficiency.

1. Introduction

Owing to the discharged toxic organic pollutants and coloured wastewater, the water bodies in nature are seriously damaged, which is harmful to human health and the environment [1, 2]. Photocatalysis, an efficient and environmental friendly technique, has shown enormous potential applications for the complete decomposition of toxic chemicals in the water, which also meet with the energy problems of the 21st century [3, 4]. Many researchers have concentrated on semiconductor photocatalysts due to their adjustable band gaps for excitation and efficient photocatalytic activities on the decomposition of organic dyes. Up to now, various oxide semiconductors have been used as photocatalysts in pollutant degradation and water splitting reactions, such as TiO_2, ZnO, WO_3, SnO_2, and CeO_2 [5–7]. However, the efficiency of photocatalytic decomposition is greatly dependent on the utilization of solar energy and the recombination of photogenerated electron-hole pairs [8]. Thus, the design and fabrication of efficient photocatalysts is an essential and challenging issue. Recently, a prospective way that combining two kinds of semiconductor photocatalysts has been widely used to enlarge the light absorption and reduce the recombining of electrons and holes. Typical examples are BiOCl/BiOI [9], NiO/ZnO [10], Ag_2O/TiO_2 [11], Ag_2O/Bi_2O_3 [12], and so on.

ZnO is an important semiconductor material with a band gap of 3.37 eV at room temperature and its photocatalytic activity has been widely explored and reported [13, 14]. However, the wide band gap of ZnO leads to the main absorption of UV light, which accounts for only 5% of the solar energy. Therefore, to improve the photocatalytic activity, it is necessary to modify ZnO by enlarging the light absorption and reducing the recombination of photoinduced carriers. Bismuth oxide (β-Bi_2O_3) is a kind of semiconductor with a band gap of 2.47 eV, which is active under visible light irradiation [15]. Studies for ZnO/Bi_2O_3 composite photocatalysts have been reported [16, 17]. For example, through the hydrothermal method, Balachandran and Swaminathan prepared heterostructured ZnO/Bi_2O_3 which showed improved activity on the photodegradation of Acid Black 1 [16]. Also Li et al. synthesized ZnO-Bi_2O_3 mixtures by microsphere

lithography technique for the degradation of methyl orange dye [17]. However, to the best of our knowledge, there is no report on the synthesis and photocatalytic evaluation of ZnO/Bi_2O_3 nanofiber composites.

In this work, the ZnO/Bi_2O_3 nanofiber composites were fabricated through an electrospinning technique and collected as nanofibrous mats. Photodecolorization measurements of RhB dye confirmed that the composite nanofibers showed greatly improved activity under both UV and visible light irradiations. The possible photocatalytic mechanisms were also discussed.

2. Experimental

2.1. Materials. Polyvinylpyrrolidone (K30) (PVP, M_w = 10000), analytical pure of zinc acetate hydrate ($Zn(CH_3COO)_2{\cdot}2H_2O$), bismuth nitrate oxide ($Bi(NO_3)_3{\cdot}5H_2O$), and ethanol were purchased from Tianjin, China Chemical Co., Ltd.

2.2. Synthesis of ZnO/Bi_2O_3 Composite Nanofibers. The polyvinylpyrrolidone (PVP) was a kind of polymer with good physiological compatibility and low toxicity. 13 g PVP powder was added into 10 mL ethanol with vigorous stirring, forming the homogeneous PVP solution. ZnO/Bi_2O_3 composite nanofibers with different molar ratios of $Zn^{2+}:Bi^{3+}$ (11 : 1 to 30 : 1) were prepared by a simple electrospinning (PVP-metal ions solutions) method. Taking the molar ratio of 11 : 1 as an example, the precursor solution was prepared by adding 0.3 g of $Bi(NO_3)_3{\cdot}5H_2O$ into 10 mL 1 M of HNO_3 to restrain the hydrolysis process and dissolving 1.5 g $ZnAc_2$ with continuous agitating for 2 h at room temperature. Then, the PVP and the precursor solutions were mixed together and stirred for 16 h to obtain the viscous spinning composite-solution.

For electrospinning, the resulting glutinous hybrid solution was breathed into the electrospinning apparatus by a vitreous syringe. The spinneret needle with an outward diameter of 1 mm was placed 10 cm away from the collector. A 20 kV voltage was applied between the collector and the needle tip. As obtained fibrous composite on the collector was dried at 60°C for 2 h and then collected. To acquire the composite nanofibers, the precursor fibers were calcined in air at 550°C for 2 h with a heating rate of 2°C min^{-1}. The obtained sample with a $Zn^{2+}:Bi^{3+}$ molar ratio of 11 : 1 was marked as Z11. Similarly, different composite samples prepared in the different contents of Zn^{2+} and Bi^{3+} for 15 : 1, 23 : 1, 25 : 1, and 30 : 1 were labeled as Z15, Z23, Z25, and Z30, respectively.

2.3. Characterization. The morphology of the electrospun composite fibers was characterized by a field emission scanning electron microscope (FE-SEM, Hitachi S-4800). The thermal decomposition process of the precursors was investigated by thermogravimetric analysis/differential thermal analysis (TGA-DTA) using a TA SDT 2960 instrument. It was performed in air from 40 to 1000°C with a heating rate of 10°C min^{-1} and flow rate of 100 mL min^{-1}. X-ray diffraction (XRD) measurement was carried out using a Rigaku D/max-2600/PC spectrometer with Cu Kα radiation in the 2θ range of 30–80°. The UV-Vis diffuse reflectance spectra (DRS) were obtained by a Shimadzu UV-2550 spectrophotometer and the wavelength range was changed from 220 nm to 700 nm.

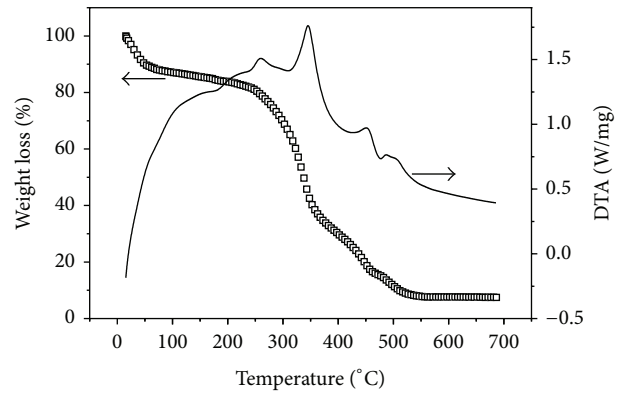

Figure 1: Synchronous TG and DTA analyses for the Z23 nanofibers.

Photocatalytic decomposition of the RhB aqueous solution (1.0×10^{-5} M, 60 mL) was performed for activity evaluation. For each sample, 60 mg catalyst was magnetically agitated for 30 min in dark to allow equilibrated adsorption-desorption of RhB on the photocatalyst surface. Then the suspension solution was irradiated in a photoreaction apparatus, and a 300 W Xe lamp was used as the light source with a filter (>420 nm). As for the UV-light excited photocatalytic process, band-pass filter (centered at 350 nm) was used to obtain the UV light. At given intervals of illumination, 4 mL of the reaction solution with catalysts was taken out during the whole process. The suspensions were centrifuged and then analyzed by a Perkin-Elmer Lambda-35 UV-Vis spectrometer.

3. Results and Discussion

In order to determine the suitable annealing temperature to get ZnO/Bi_2O_3 composite nanofibers, the thermal behavior of the precursor was tested. Figure 1 showed the typical results of synchronous TG and DTA analyses for the hybrid precursor of Z23. The differential thermal analysis (DTA) curve showed broad exothermic peaks below 300°C, which could be associated with the loss of moisture and trapped solvent ethanol and carbon dioxide [10]. A weight loss of ~20% was observed at the corresponding temperature range in TG curve. Further, the pyrolysis of PVP by a dehydration on the polymer side chain and the disintegration of zinc acetate and bismuth nitrate occurred between 300°C and 500°C, accompanied by a continuous weight loss of ~70% [18, 19]. The exothermic peaks at about 363, 463, and 500°C in the DTA curve were attributed to the decomposition of zinc acetate, bismuth nitrate oxide, and the main chain of PVP, respectively. There was no obvious weight loss after 500°C, which verified that the precursor was completely decomposed and ZnO/Bi_2O_3 composite formed. Therefore,

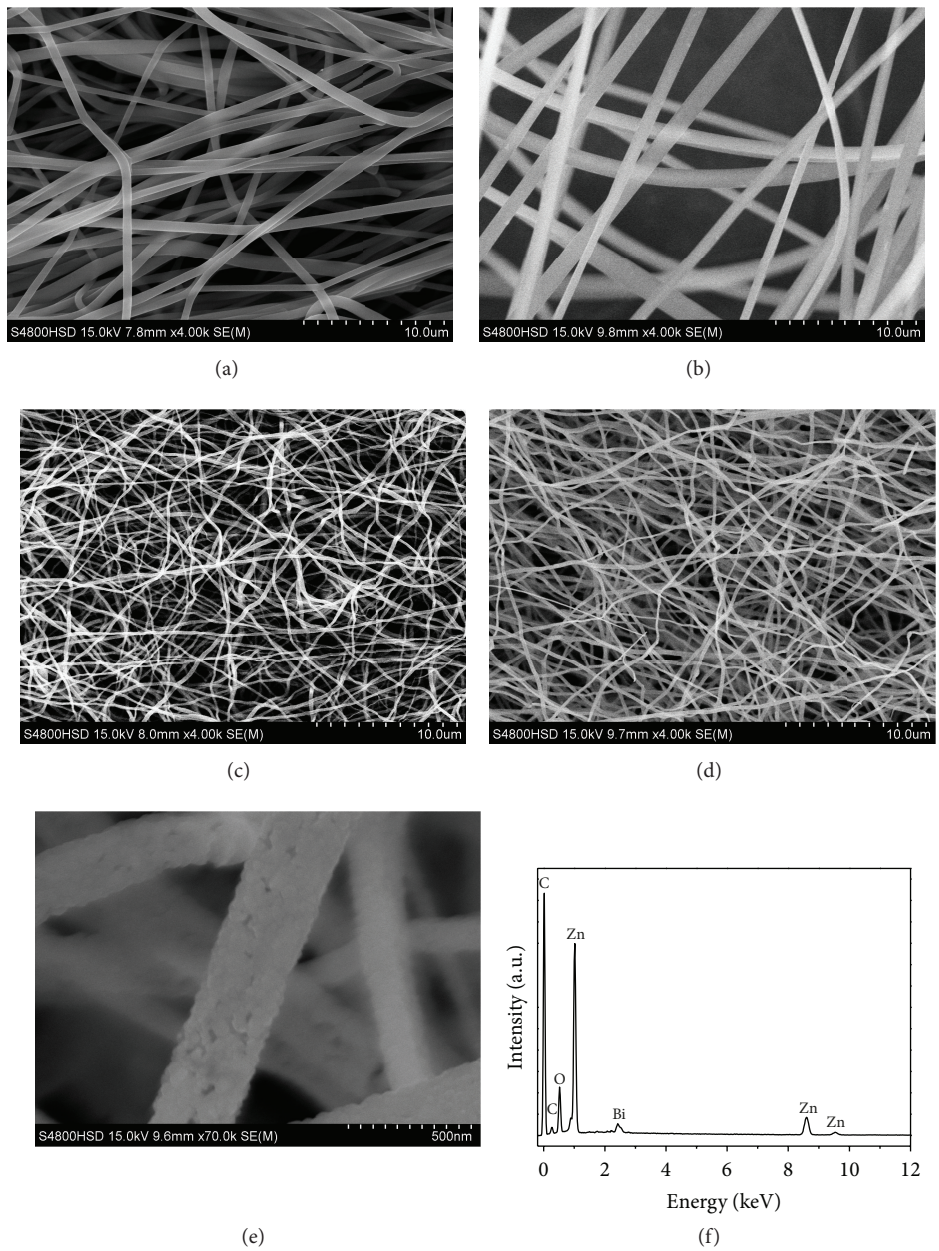

Figure 2: SEM images of (a) as-spun precursors Z11 and (b) Z23, (c) annealed nanofibers Z11 and (d) Z23, (e) high magnification view of Z23 nanofibers, and (f) EDX spectrum of Z23.

the calcination temperature for precursor fibers was selected as 550°C in order to obtain the composite fibers.

In order to obtain the microstructure information, SEM observations of the precursor and calcined nanofibers were carried out and the images are given in Figure 2. Before the annealing treatment, the morphology of as-spun composite nanofibers Z11 and Z23 in Figures 2(a) and 2(b) showed that the diameters of nanofibers were in the range of 700–900 nm with a relatively smooth surface. After annealing, the nanofibers maintained the continuous fiber structure, whilst the diameter of composite nanofibers of Z11 and Z23 (Figures 2(c), and 2(d)) was reduced to 100–200 nm. High-magnified image of sample Z23 (Figure 2(e)) showed that the surface of the annealed nanofibers turned to be rough and porous. The energy-dispersive X-ray fluorescence (EDX) spectrum (Figure 2(f)) taken from Z23 confirmed the existence of C, O, Bi, and Zn elements in the nanofibers. The EDX spectrum further indicated that the composite nanofibers were fabricated.

XRD patterns of the calcined nanofibers are shown in Figure 3. The crystal planes of (100), (002), (101), (102), (110), (103), (200), (112), and (201) from the ZnO wurtzite (JCPDS 36-1451) were observed in the patterns for all samples and the characteristic crystalline peaks of ZnO showed no obvious change in theses samples. ZnO also presented good crystallinity in the composite nanofibers, as confirmed by

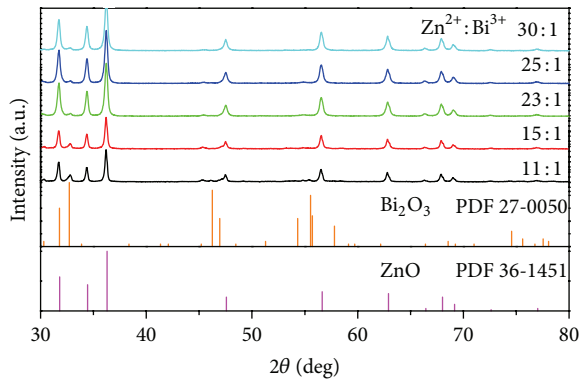

Figure 3: XRD diffraction patterns for the ZnO/Bi_2O_3 composite nanofibers with variable $Zn^{2+}:Bi^{3+}$ ratios.

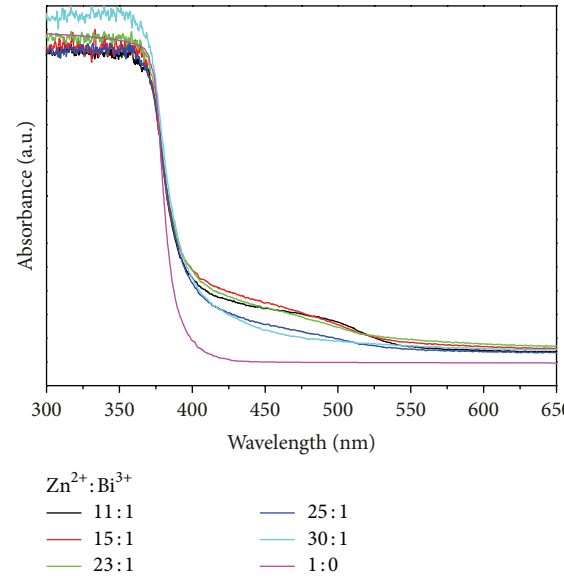

Figure 4: DRS spectra of the ZnO/Bi_2O_3 nanofibers with variable $Zn^{2+}:Bi^{3+}$ ratios.

the sharp diffraction peaks. The diffraction peaks of β-Bi_2O_3 (JCPDS 27-0050) were also observed in each sample and slightly varied due to the different contents of Bi_2O_3. It showed that the intensity of diffraction peaks of β-Bi_2O_3 turned to be stronger with increase content in the composite. No characteristic peaks of impurities such as ZnO_2, BiO_2, and Bi_4O_7 were discovered, suggesting that the nanofibers composed of ZnO and Bi_2O_3 phases.

The DRS spectra of the ZnO/Bi_2O_3 nanofibers were shown in Figure 4. It can be seen that all the composites exhibited the similar absorption edge below 400 nm, while an obvious visible light absorption band around 400–550 nm was observed and striking red shifts with the elevating content of β-Bi_2O_3 were observed for the composites, due to the narrow band gap of β-Bi_2O_3 (~2.47 eV) compared with that of ZnO (3.37 eV). In sequence, the ability of light absorption in the visible range for the composites catalysts is as follows: ZnO < Z30 < Z25 < Z11 < Z15 < Z23.

The photocatalytic activities of the ZnO/Bi_2O_3 nanofibers were demonstrated for the degradation of organic pollutants Rhodamine B (RhB) irradiated with both UV and visible light (Figures 5(a), and 5(b)), respectively. The characteristics of Rhodamine B were provided in Table 1. The photodegradation process was measured by monitoring the absorbing band of RhB at 554 nm. The photodegradation efficiency is defined as the C/C_0, where C_0 (1.0×10^{-5} M) is the initial concentration and C is the concentration of RhB at intervals. Under visible illumination (Figure 5(a)), the time required to decolorize 85% of the RhB was 180 min by using the Z23 composite nanofibers catalyst, which was much shorter than the other nanofibers in our experiment. For comparison, the direct photolysis of RhB without catalyst was tested and only 10% of organic dye was degraded at 180 min. The results illustrated that the ZnO/Bi_2O_3 composite nanofibers presented good visible light responsive activity for the photodegradation of RhB. Since ZnO presents no absorption of visible light from DRS, there is no photodegradation of RhB on ZnO under visible light excitation. Moreover, the photocatalytic activities of ZnO/Bi_2O_3 nanofibers under UV light were shown in Figure 5(b). The Z23 photocatalyst also exhibited the highest photocatalytic activity and nearly

Table 1: The characteristics of Rhodamine B.

	Molecular formula	Molar mass	Maximum absorption peak
Rhodamine B	$C_{28}H_{31}ClN_2O_3$	479.02	554 nm

95% of RhB was decomposed after 90 min under UV-light irradiation. Typical evolution of RhB absorption spectra for Z23 nanofiber under UV light was inserted in Figure 5(b). The maximum absorption spectra of RhB with the characteristic adsorption peak at 554 nm shifted to 490 nm and decreased obviously with the increase in the exposed duration in approximately 90 min. The formation of the intermediates leads to the hypsochromic shift of the maximum absorption band [20]. This also confirmed that the decomposition of RhB took place by the photocatalysis of the nanofibers.

To better interpret the mechanisms of the enhanced photocatalytic activity for ZnO/Bi_2O_3 composites, a schematic band structure was given in Figure 6. It is well known that ZnO (E_g = 3.37 eV) can only be photoactivated by the ultraviolet excitation, while Bi_2O_3 (E_g = 2.47 eV) can absorb visible light with wavelength <500 nm. In our photocatalytic experiments, both UV and visible light induced photocatalysis process were observed in the degradation of RhB over the ZnO/Bi_2O_3 composite nanofibers and the Z23 composite exhibited the highest photocatalytic activity. The possible photocatalytic process can be described as follows:

$$(ZnO/Bi_2O_3) + h\nu \longrightarrow (ZnO/Bi_2O_3)(e_{CB}^- + h_{VB}^+) \quad (1)$$

$$RhB + h\nu \longrightarrow RhB^* + e_{CB}^- \quad (2)$$

$$e_{CB}^- + O_2 \longrightarrow {}^{\bullet}O_2^- \quad (3)$$

$$h_{VB}^+ + H_2O \longrightarrow H^+ + {}^{\bullet}OH \quad (4)$$

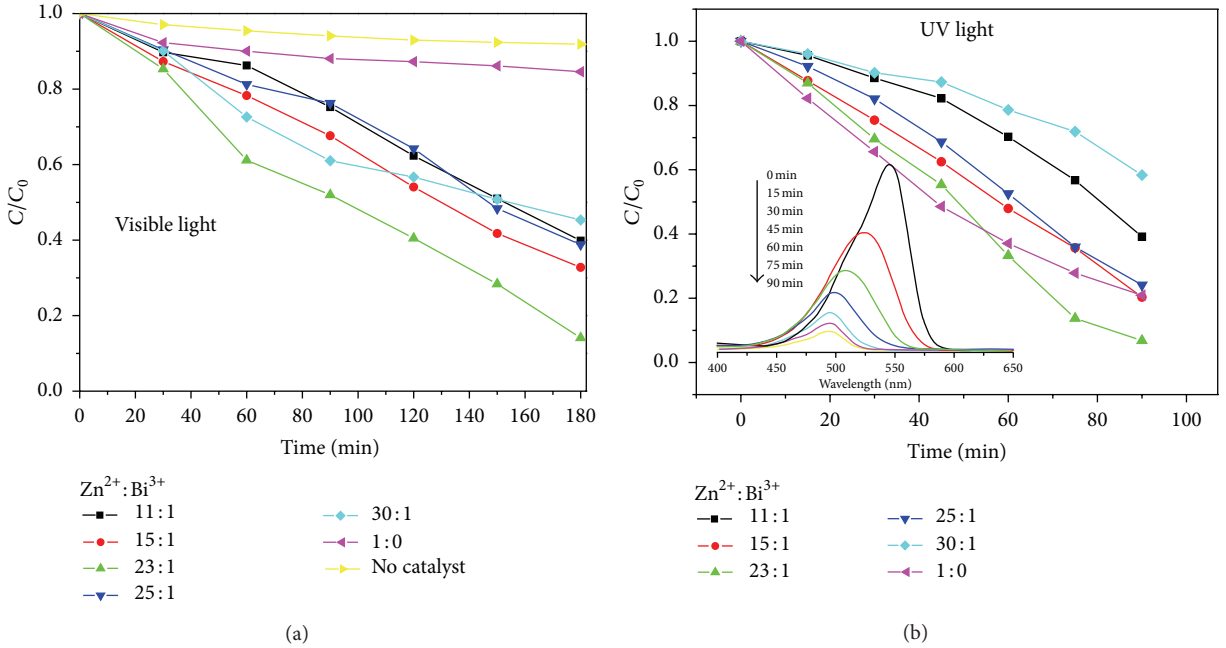

Figure 5: Photocatalytic degradation of RhB in the presence of ZnO/Bi_2O_3 nanofibers under (a) UV and (b) visible light excitation. The concentration of RhB was 1.0×10^{-5} M and 60 mg catalyst was added in 60 mL RhB solution.

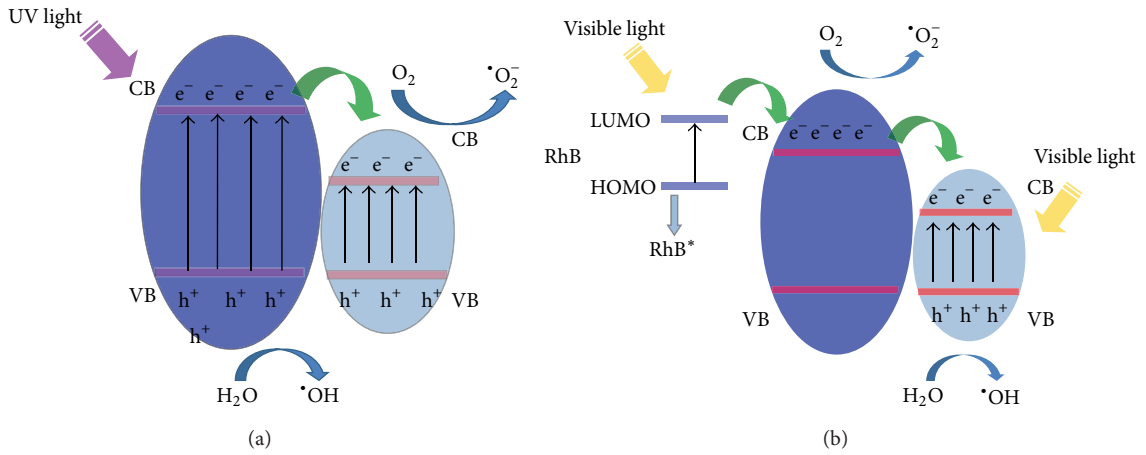

Figure 6: Schematic diagram for the band structure and electron-hole separations in both semiconductors for (a) UV light excitation and (b) visible-light excitation process.

$$2^{\bullet}O_2^- + 2H_2O \longrightarrow H_2O_2 + O_2 + 2OH^- \quad (5)$$

$$H_2O_2 + e_{CB}^- + H^+ \longrightarrow {}^{\bullet}OH + OH^- \quad (6)$$

$$RhB + h_{VB}^+ / {}^{\bullet}OH / {}^{\bullet}O_2^- \longrightarrow CO_2 + H_2O + \text{other minerals} \quad (7)$$

Under the UV light excitation, photoinduced electrons and holes can be generated in both of the ZnO and Bi_2O_3, as demonstrated in (1). Subsequently, the electrons from the conduction band (CB) of ZnO can transfer to the CB of Bi_2O_3 due to the energy matching of CB in the composite, which also greatly inhibited the recombination of photoexcited carriers. The efficient separation between the electrons and holes at the interface of the two semiconductors promoted the photocatalytic performance of the ZnO/Bi_2O_3 nanofibers, as shown in Figure 6(a).

When being under the visible light excitation, only Bi_2O_3 in the composite can absorb the light above 420 nm to generate photoinduced carriers, indicating that there are other reasons for the photocatalytic degradation of RhB, as shown in Figure 6(b). The RhB dye used in this study can also be excited by the visible light with photogenerated electrons from the highest occupied molecular orbital (HOMO) up to the lowest unoccupied molecular orbital (LUMO), producing the singlet and triplet excited states (RhB^*) (2). Electrons

from the RhB dye would be injected to the CB of ZnO, and subsequently the excited electrons on ZnO transferred to the CB of Bi_2O_3 [17]. The photogenerated electrons and holes transferred to the surface and reacted with the adsorbed reactants in an analogous process with the UV-light photocatalytic reaction. The photoinduced holes (trapped by H_2O) produced hydroxyl radical species ($^{\bullet}OH$) and the photoinduced electrons (trapped by O_2 and H_2O) produced hydroxyl radical species ($^{\bullet}OH$), which are extremely strong oxidants for the degradation of organic chemicals (3) to (7) [17, 21]. So based on the discussion above, the mechanisms for the UV and visible light photocatalytic processes were considered as direct photocatalysis and photosensitization, respectively.

4. Conclusions

In summary, ZnO/Bi_2O_3 composites nanofibers with diameters of 100–200 nm were synthesized using an electrospinning method and their UV and visible light responsive photocatalysis activities were evaluated. Our experimental results showed that the photodecomposition rate of RhB under both UV and visible light by the Z23 was much higher than other nanofibers within the same duration. The improvements of photocatalytic activity were ascribed to the effective separation of photoinduced electrons and hole, which presented in the direct photocatalysis and photosensitization process for the UV and visible light excitation photocatalytic measurements.

Conflict of Interests

The authors declare that there is no conflict of interests regarding the publication of this paper.

Acknowledgments

The work was sponsored by the National Science Foundation of China (51102069). This work was also partly supported by foundation from Heilongjiang Provincial Committee of Education (1253G036, JG2012010370) and Open Project from Key Laboratory for Photonic and Electronic Bandgap Materials of Ministry of Education (PEBM 201209).

References

[1] R. Michael, S. T. M. Hoffmann, W. Choi, and D. W. Bahnemannt, "Environmental applications of semiconductor photocatalysi," *Chemical Reviews*, vol. 95, no. 1, pp. 69–94, 1994.

[2] P. A. Pekakis, N. P. Xekoukoulotakis, and D. Mantzavinos, "Treatment of textile dyehouse wastewater by TiO_2 photocatalysis," *Water Research*, vol. 40, no. 6, pp. 1276–1286, 2006.

[3] C. Kim, M. Choi, and J. Jang, "Nitrogen-doped SiO_2/TiO_2 core/shell nanoparticles as highly efficient visible light photocatalyst," *Catalysis Communications*, vol. 11, no. 5, pp. 378–382, 2010.

[4] S. C. Roy, O. K. Varghese, M. Paulose, and C. A. Grimes, "Toward solar fuels: photocatalytic conversion of carbon dioxide to hydrocarbons," *ACS Nano*, vol. 4, no. 3, pp. 1259–1278, 2010.

[5] O. Carp, C. L. Huisman, and A. Reller, "Photoinduced reactivity of titanium dioxide," *Progress in Solid State Chemistry*, vol. 32, no. 1-2, pp. 33–177, 2004.

[6] X. Duan, G. Wang, H. Wang, Y. Wang, C. Shen, and W. Cai, "Orientable pore-size-distribution of ZnO nanostructures and their superior photocatalytic activity," *CrystEngComm*, vol. 12, no. 10, pp. 2821–2825, 2010.

[7] A. Kudo, H. Kato, and I. Tsuji, "Strategies for the development of visible-light-driven photocatalysts for water splitting," *Chemistry Letters*, vol. 33, no. 12, pp. 1534–1539, 2004.

[8] C. J. Lin, Y. H. Yu, and Y. H. Liou, "Free-standing TiO_2 nanotube array films sensitized with CdS as highly active solar light-driven photocatalysts," *Applied Catalysis B*, vol. 93, no. 1-2, pp. 119–125, 2009.

[9] T. B. Li, G. Chen, C. Zhou, Z. Y. Shen, R. C. Jin, and J. X. Sun, "New photocatalyst BiOCl/BiOI composites with highly enhanced visible light photocatalytic performances," *Dalton Transactions*, vol. 40, no. 25, pp. 6751–6758, 2011.

[10] C. Shao, X. Yang, H. Guan, Y. Liu, and J. Gong, "Electrospun nanofibers of NiO/ZnO composite," *Inorganic Chemistry Communications*, vol. 7, no. 5, pp. 625–627, 2004.

[11] W. Zhou, H. Liu, J. Wang, D. Liu, G. Du, and J. Cui, "Ag_2O/TiO_2 nanobelts heterostructure with enhanced ultraviolet and visible photocatalytic activity," *ACS Applied Materials and Interfaces*, vol. 2, no. 8, pp. 2385–2392, 2010.

[12] L. Zhu, B. Wei, L. L. Xu et al., "Ag_2O-Bi_2O_3 composites: synthesis, characterization and high efficient photocatalytic activities," *CrystEngComm*, vol. 14, no. 18, pp. 5705–5709, 2012.

[13] C. Hariharan, "Photocatalytic degradation of organic contaminants in water by ZnO nanoparticles: revisited," *Applied Catalysis A*, vol. 304, no. 1-2, pp. 55–61, 2006.

[14] C. A. K. Gouvêa, F. Wypych, S. G. Moraes, N. Durán, and P. Peralta-Zamora, "Semiconductor-assisted photodegradation of lignin, dye, and kraft effluent by Ag-doped ZnO," *Chemosphere*, vol. 40, no. 4, pp. 427–432, 2000.

[15] Y. Qiu, M. Yang, H. Fan et al., "Nanowires of α- and β-Bi_2O_3: phase-selective synthesis and application in photocatalysis," *CrystEngComm*, vol. 13, no. 6, pp. 1843–1850, 2011.

[16] S. Balachandran and M. Swaminathan, "Facile fabrication of heterostructured Bi_2O_3-ZnO photocatalyst and its enhanced photocatalytic activity," *The Journal of Physical Chemistry C*, vol. 116, no. 50, pp. 26306–26312, 2012.

[17] C. Li, J. Zhang, J. Yang, T. Wang, X. Lv, and Z. Tang, "Methods to improve the photocatalytic activity of immobilized ZnO/Bi_2O_3 composite," *Applied Catalysis A*, vol. 402, no. 1-2, pp. 80–86, 2011.

[18] X. Yang, C. Shao, H. Guan, X. Li, and J. Gong, "Preparation and characterization of ZnO nanofibers by using electrospun PVA/zinc acetate composite fiber as precursor," *Inorganic Chemistry Communications*, vol. 7, no. 2, pp. 176–178, 2004.

[19] M.-G. Ma, J.-F. Zhu, R.-C. Sun, and Y.-J. Zhu, "Microwave-assisted synthesis of hierarchical Bi_2O_3 spheres assembled from nanosheets with pore structure," *Materials Letters*, vol. 64, no. 13, pp. 1524–1527, 2010.

[20] E.-J. Li, K. Xia, S.-F. Yin, W.-L. Dai, S.-L. Luo, and C.-T. Au, "Preparation, characterization and photocatalytic activity of Bi_2O_3-MgO composites," *Materials Chemistry and Physics*, vol. 125, no. 1-2, pp. 236–241, 2011.

[21] L. Wu, J. C. Yu, and X. Fu, "Characterization and photocatalytic mechanism of nanosized CdS coupled TiO_2 nanocrystals under visible light irradiation," *Journal of Molecular Catalysis A*, vol. 244, no. 1-2, pp. 25–32, 2006.